Progress report on air bearing slumping of thin glass mirrors for x-ray telescopes

Mark L. Schattenburg*[a], Brandon Chalifoux[b],
Michael D. DeTienne[c], Ralf K. Heilmann[a], Heng Zuo[d]
[a]Space Nanotechnology Lab, MIT Kavli Institute, Cambridge, MA, USA 02139
[b]MIT Dept. of Mechanical Engineering, Cambridge, MA, USA 02139
[c]MIT Dept. of Electrical Engineering, Cambridge, MA, USA 02139
[d]MIT Dept. of Aero/Astro Engineering, Cambridge, MA, USA 02139
*marks@space.mit.edu; phone: (617) 253-3180; snl.mit.edu

ABSTRACT

The successful NuSTAR telescope was fabricated with thin glass mirrors formed into conic shapes by thermal slumping of thin glass sheets onto high precision mandrels. While mirrors generated by this process have very good figure, the best mirrors to date have a resolution limited to ~7 arc sec, due primarily to mid-range scale spatial frequency errors. These mid-range errors are believed to be due to clumping and particulates in the anti-stick coatings used to prevent sticking between mandrel and mirrors. We have developed a new slumping process which avoids sticking and surface-induced mid-range error by floating hot glass substrates between a pair of porous air bearing mandrels through which compressed nitrogen is forced. We report on the design and testing of an improved air bearing slumping tool and show results of short and long slumping cycles.

Keywords: x-ray mirrors, slumping, glass, air bearings

1. INTRODUCTION

Recent progress in high-resolution x-ray mirror technology has brought within reach a powerful new x-ray telescope concept—the X-ray Surveyor [1]. This proposed mission would have comparable angular resolution to Chandra but with some 30 times the collecting area, a much wider field of view, and spectrometers with many times improved spectral resolution. NASA has recently called for community study of such a mission for consideration by the 2020 Decadal Survey. An X-ray Surveyor would address a broad range of science questions and thus has an excellent chance of appealing to a broad swath of the astrophysics community.

In order for this mission concept to move forward, it is absolutely essential to demonstrate the proposed lightweight 0.5 arc-second telescope optics. Unfortunately, the current state of technology allows a convincing demonstration only for a ~10 arc sec telescope [2, 3]. While the field is rapidly progressing, the required 20X improvement in resolution demands a re-doubling of effort and could benefit from fresh perspectives and alternative approaches.

A number of groups in the US, Europe and Japan are pursuing innovations in lightweight high resolution x-ray telescopes. These technologies can be divided into three basic categories: pore optics, full shell optics and segmented optics. A review by O'Dell *et al.* summarizes the different approaches [2].

Pore optics are being pursued in Europe for the Athena mission [4]. This technology uses machined and bonded silicon wafers to form an array of pores which concentrate x-rays to a focal spot. Pore optics have the advantage of light weight, but progress towards Athena's goal of 5 arc sec has been slow. Diffraction from pores also limits the ultimate resolution.

Full shell optics utilize thin ring-shaped shells of glass [5], metal [6], ceramics, composites or other materials [7]. While these technologies are promising, they may be difficult to scale to the 3 m aperture of an X-ray Surveyor.

Segmented optics utilize small rectangular mirrors (ranging from 100-300 mm on a side) which are shaped into Wolter conic curves and then assembled into wedge-shaped modules. These modules are then assembled into the full telescope aperture [1, 3, 8]. Many consider this approach promising for the Surveyor concept, mainly because of the modular design's scalability.

Thermal shaping (or slumping) of thin glass substrates for segmented mirrors is being developed in the US [3, 9] and Europe [10, 11]. This proven thin-glass shaping technology was used to produce mirrors for the very successful NuSTAR mission [12], which features a telescope with an angular resolution close to one arc minute. Technology for slumping NuSTAR glass mirrors was originally developed by teams at Columbia University and the Lawrence Livermore National Lab which was then further refined for mass production by a group at NASA Goddard Space Flight Center (GSFC). The GSFC group has further advanced this technology towards higher resolution, improving all aspects of thin segmented mirror technology, including mandrel fabrication, thermal shaping, metrology and mirror assembly. A group at NASA Marshall Space Flight Center (MSFC) has also made significant contributions, including the development of low-stress coatings [13]. Best x-ray test results to date for an assembled module with three-mirror pairs is about 8.3 arc sec, which should be sufficient for a 10 arc sec telescope [3].

The thermal forming method developed by the GSFC group is illustrated in Fig. 1a (different approaches are being pursued in Europe). A thin, flat piece of Schott D263 glass is placed on a precision mandrel which is then heated in an oven to a temperature near the glass softening point (~600 C). The softened glass deforms under gravity load to conform to the shape of the mandrel with high precision. The furnace is then slowly cooled and the mirror released. A powder-based anti-stick coating is applied to the mandrel to prevent the hot glass from sticking. While this process results in mirrors with excellent fidelity over long spatial wavelengths, the RMS surface error is currently dominated by mid-range spatial frequencies due to clumping and impurities in the anti-stick coating [9, 14]. The process also requires lengthy thermal cycles of up to two days per mirror in order to achieve the highest fidelity replication.

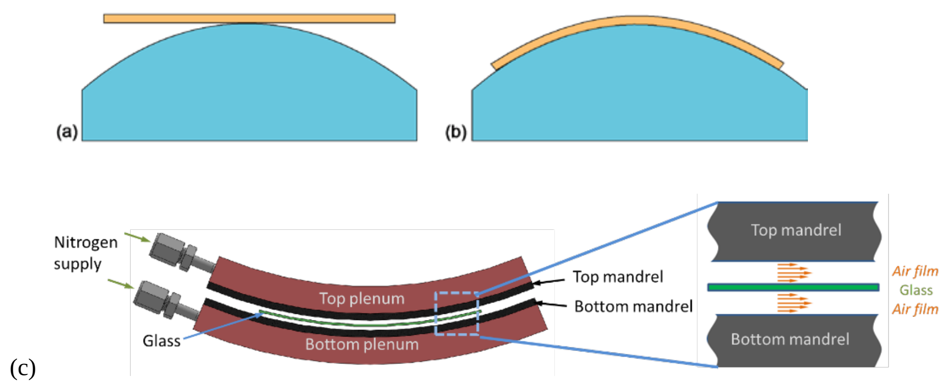

Figure 1. (a) Depiction of GSFC thermal slumping process used to produce NuSTAR mirrors. A flat glass sheet (a) is thermally softened and slumped over a precision mandrel (b). (c) Thermal slumping process developed at MIT. Glass is slumped against thin cushions of air generated by a pair of pressurized porous mandrels.

Our laboratory has recently developed an alternative approach for thin glass slumping that seeks to avoid the mid- and high-spatial frequency surface errors that plague conventional approaches [15, 16]. Glass sheets are slumped between thin cushions of air (10-50 μm thick) generated by opposing pairs of pressurized porous ceramic mandrels (see Fig. 1b). While the fidelity over long spatial wavelengths is not as good as achieved with the GSFC approach, the resulting mirrors are devoid of the mid-range errors caused by the anti-stick coating. We have proposed to correct residual long-range errors after slumping using a deterministic figure correction scheme such as ion-implant stress or differential deposition (see Fig. 2) [6, 16, 17].

Mid-range spatial frequency errors in thin optics pose a serious impediment to further progress towards sub-arc sec telescopes. Mid-range errors are difficult to correct by proposed post-figure correction schemes, including active methods such as PZT actuated mirrors [18]. We believe that a mirror figuring approach based on air-bearing slumped glass is capable of producing mirrors with low mid-range errors, which we believe will be essential for success with all proposed post-figure correction schemes.

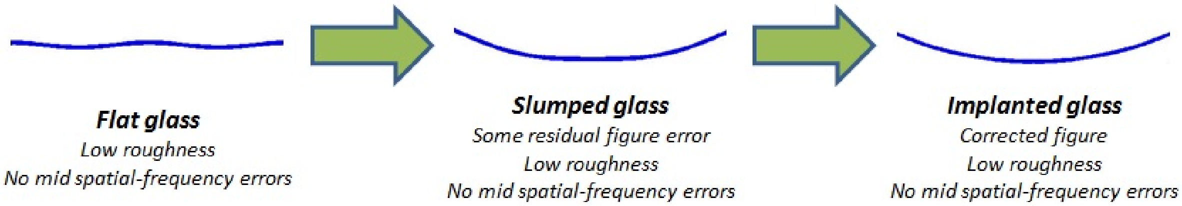

Figure 2. Proposed mirror fabrication process. Flat glass is slumped to achieve a figure close to the desired shape, but with very low mid-range spatial frequency errors. A deterministic post-figure correction technique such as ion implant or differential deposition is used to correct remaining figure errors.

2. RECENT PROGRESS WITH AIR BEARING SLUMPING

Recent effort in our lab has focused on improving the reliability and control of our current flat substrate slumping tool, shown in Fig. 3. This tool was designed as a test bed for exploring various control strategies and sensor/actuator concepts. Since the glass floats on a film of air, it is inherently unstable and needs to be somehow manipulated to stay in the bearing. The control system's job is to maintain the glass sheet near the bearing center during the entire thermal cycle. This task is challenging due the high temperatures (up to 600 C), rapid thermal cycles (20 C to 600 C and back in just a few hours), and 24/7 operation, requiring repetition of this process several times a day for many weeks or months. This challenge was sufficiently difficult that we elected to develop and debug the process first using flat substrates. Flats are also much easier to work with and measure and the bearings are less costly to fabricate. We plan to use lessons-learned in the flat substrate campaign to apply to future tools that will slump the curved optics of Wolter-type mirrors. In Section 4 we discuss a prototype tool for slumping curved optics which is now being built and tested.

Significant progress has been made in a number of technical areas, including a completely re-designed bearing assembly, development of more accurate and reliable sensors and actuators, more precise bearing gas flow controls, and improved control algorithms. These have resulted in a number of benefits, including much higher system reliability, fewer glass "crash" events, quicker slumping cycles, and more consistent run-to-run results. Here we discuss these improvements in detail as well as present some recent results.

(a)
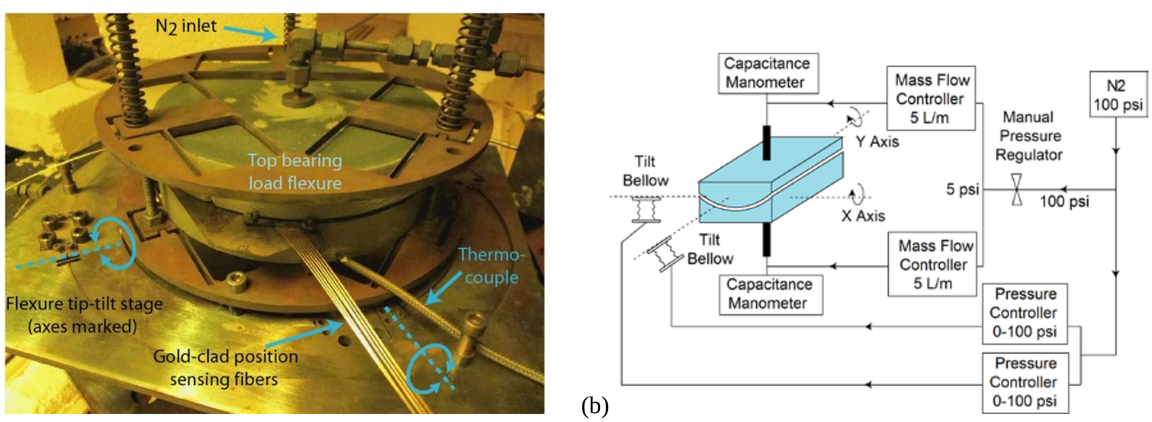

Figure 3. (a) Photograph of slumping tool with view of top mandrel and load plate, tip-tilt flexure stage, and mirror position fiber sensors. (b) Depiction of slumping tool nitrogen gas control system. Top and bottom bearing plenum pressures are measured with capacitance manometers and controlled using mass flow controllers. The position of the floating sheet in the bearing is controlled by tilting the bearing around the X and Y axes. High temperature Inconel bellows fed by pressure controllers tilt the bearing to control the glass position. LabVIEW software provides digital control of the tool.

The slumping system shown in Fig. 3 utilizes a pair of porous silicon carbide mandrels, each mandrel comprised of a precision flat-ground bearing plate bonded to a plenum cavity using a high temperature adhesive. Fig. 4a shows a broken mandrel revealing the plenum cavity which is fed pressurized nitrogen by a stainless steel inlet. The tool software controls mirror position in the bearing by using a simple two-axis tip-tilt technique (see Fig. 3a). Mirror position is measured using a fiber-based position sensing method (see Fig. 4b). Bearing tilt is performed with a two-axis flexure tip-tilt stage actuated by high-temperature Inconel bellows. Pressure actuators are used to control the extension of X and Y tilt bellows (see Fig. 3b). The pressure in the top and bottom bearings is measured by capacitance manometers and controlled using mass flow controllers. Since the viscosity of air changes by ~2.5X between room temperature and 600 C, the flow rate needs to be constantly adjusted to achieve the target bearing pressure (typically 0.01-0.05 psi). Substrate position sensing, actuation, and bearing pressure control are performed using a LabVIEW-based feedback control system.

An important recent advance was the replacement of nickel-clad fibers with gold-clad fibers. During early trials we used copper-clad fibers which became brittle after only one thermal cycle. We then developed a fiber nickel coating process which prevented copper oxidation and allowed fibers to be used for multiple slumping cycles. Eventually, however, these fibers also become brittle to the point where essentially every slumping run requires extensive fiber testing and replacement. Due to this problem, and other reliability issues, accomplishing even a single slumping run a week required a great deal of effort. Gold-clad fibers have recently become available (Fiberguide Industries) which have virtually eliminated thermal degradation and enabled quick and simple sample replacement cycles between slumping runs. It has become commonplace for us to achieve three slumping runs per day, and higher rates should be possible.

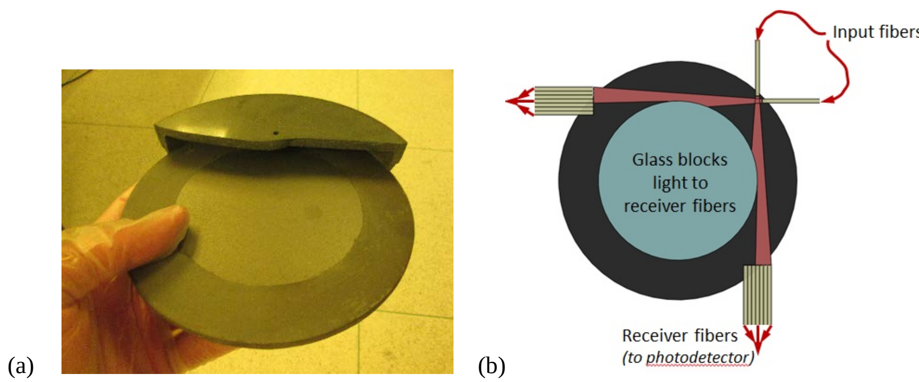

Figure 5. (a) Photograph of broken mandrel showing bearing plate and plenum cavity. The bearing and plenum are fabricated from porous silicon carbide pieces which are bonded together using a high temperature adhesive. (b) Fiber-based position sensing used in slumping tool. Input fibers deliver light to illuminate the edges of the glass substrates. A laterally moving substrate gradually blocks light from entering receiver fibers, resulting in a low-noise position measurement by measuring total received light intensity.

3. RECENT SLUMPING RESULTS

Recent improvements have enabled a large jump in the rate of slumping trials. Since June of this year, when gold fibers were first installed, we have conducted over 60 slumping runs. During these tests we used 100 mm-diameter, 550 μm-thick Schott D263 wafers. Only a snapshot of results can be presented here.

Fig. 6a shows temperature data from a six-hour run, wherein the duration of time when the glass was at the 550 C set point dwell temperature was less than an hour. It is remarkable that significant glass flattening is observed for short dwells at temperatures just slightly above D263's strain point (529 C). During slumping runs the floating substrate is normally actuated to follow a small radius circle—a process called "dithering." This technique allows direct visual confirmation of free-floating control during the entire run. Before we developed this technique, it was difficult to distinguish a mirror under control from one which had somehow become stuck at a particular positon. Fig 6b shows position data for a glass wafer taken during the peak temperature dwell.

Fig. 7a shows data obtained from a set of runs performed with 50 micron-thick gaps between glass and bearing surfaces. Surface topographs were obtained using a deep-UV Shack-Hartmann tool [19]. We observe that unslumped glass wafers typically have 50-90 microns peak-to-valley (P-V) surface height variation. Note the rapid drop of P-V for peak dwell times up to ~0.4 hour, followed by a plateau. Fig. 7b shows a Shack-Hartmann topograph of a substrate surface after a 0.4 hour slumping run. While the ~10 micron P-V is a great improvement over the initial shape, the large amount of astigmatism suggests that the run was too short, or was not hot enough to drive to steady state. Fig. 8 shows data obtained from two samples that were slumped for 16 hours with a 550 C peak temperature and 35 micron gap. A repeatable sombrero shape was obtained for both samples, suggesting that steady-state was achieved.

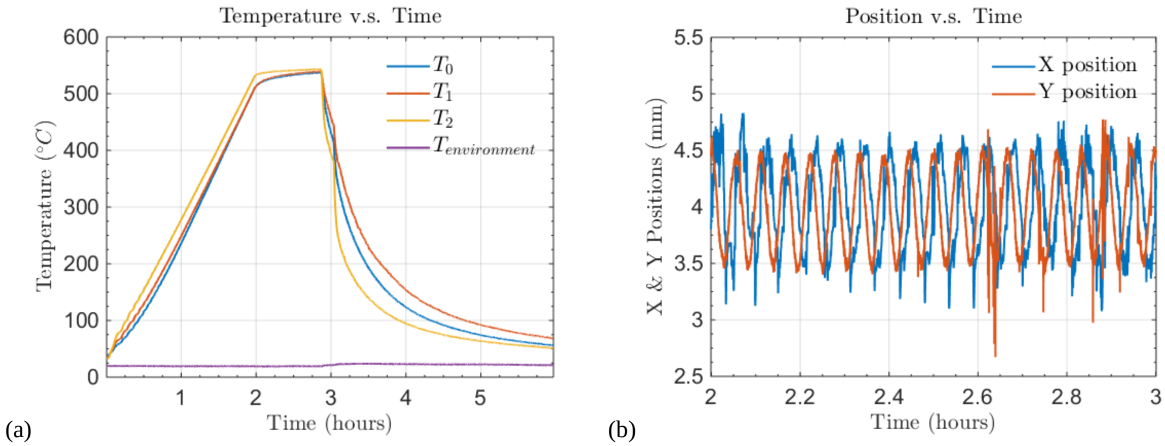

Figure 6. (a) Furnace temperature during a slumping run measured at several points near the mandrel. This particular cycle had a peak temperature of around 550 C and peak dwell time of ~0.9 hours. (b) Plot of measured mirror position in the bearing during peak temperature dwell. The control system actuates the hot substrate to follow a ~1 mm diameter "dither" circle with a period of ~3 minutes.

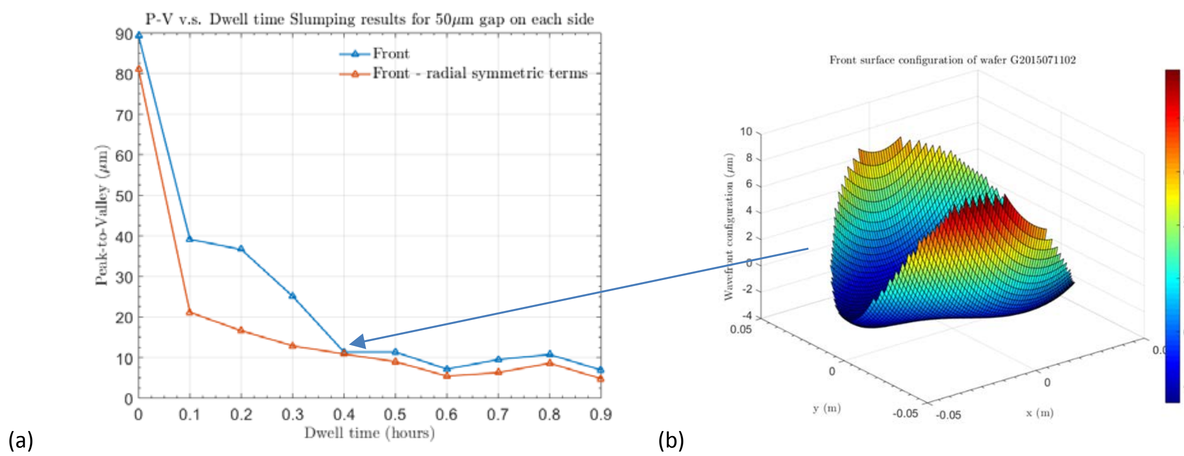

Figure 7. (a) Slumping results using a 50 micron bearing gap and a dwell point set temperature of 550 C. Each dwell time trial was performed with a different substrate. Rapid flattening occurs for dwells up to ~0.4 hour duration, which then slows for longer dwells. (b) Shack-Hartmann surface topograph of substrate after an 0.4 hour slump dwell.

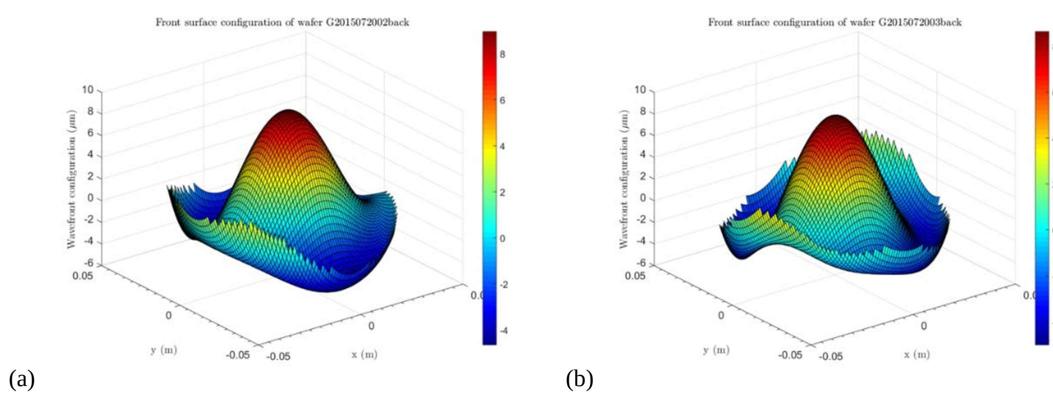

Figure 8. Topographs for substrates slumped for 16 hours using a 35 micron bearing gap and a dwell temperature set point of 550 C. (a) Sample G2015072002. (b) Sample G2015072003. Note progression of both samples to a very similar "sombrero" shape and P-V.

The steady-state dome shape which appears after long slumping runs is believed to be due to pressure dynamics in the bearing. Modelling shows that the air pressure in the gap is highest at the bearing's center and drops to zero at the rim. The high pressure in the bearing middle generates a stiff restoring force, whilst the low pressure at the rim results in a soft restoring force. Since the gravity load of the substrate is a constant, the edge is expected to sag more than the center, yielding a dome shape. We do not fully understand, however, what is causing the mirror's upward inflection at the rim.

4. SUMMARY AND NEXT STEPS

We have developed a robust air bearing slumping tool which yields repeatable steady-state shapes with a P-V of ~10 microns at a gap of 35 microns. Modelling shows that smaller gaps should result in much lower P-V numbers which we plan to pursue. The reliable design enables quick slumping runs and rapid sample changeover, achieving up to three slumping runs per day with little maintenance. During the next year we plan to continue tests with the flat slumping tool to more thoroughly explore the time-temperature-gap parameter space. These results will be used to further refine our computer model of the system. We will fold the knowledge gained during these experiments into the design of a new tool for slumping conical mirrors.

At this point the technology for slumping flat substrates has become sufficiently advanced to envision extension to conical optics. To this end we are developing a test stand for slumping conical mirrors (see Fig. 9). The tool utilizes porous graphite bearings with aluminum plenums and a tip-tilt stage for substrate position control. The tool is designed for room temperature tests of substrate position sensor and actuator concepts which need to be validated in the conical geometry. The tool will utilize NuSTAR flight spare mirrors for these tests. Lessons learned from this project will inform the design of a new tool targeted for hot slumping.

(a) (b)

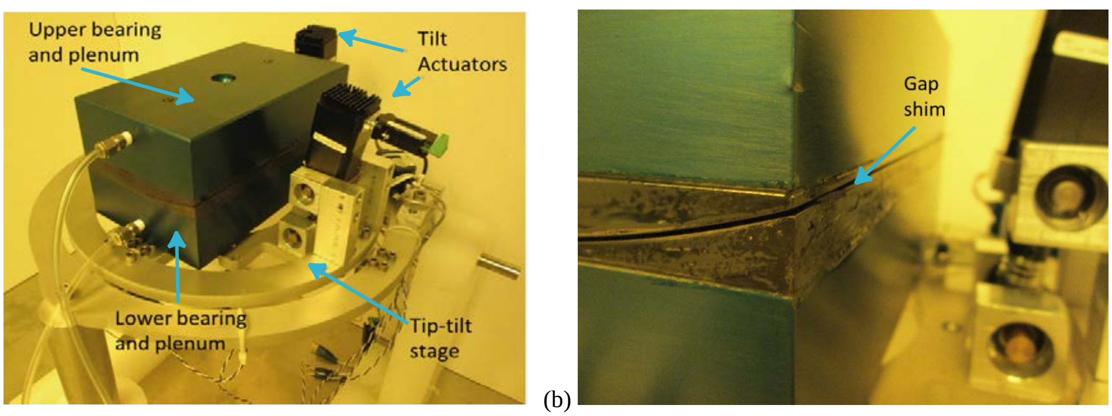

Figure 9. (a) Photograph of conical optic slumping test stand which is designed for room temperature tests. This prototype tool is designed to test substrate position sensor and control concepts in a cylindrical geometry. (b) Detail of test stand showing porous graphite air bearings, aluminum plenums and gap shims.

ACKNOWLEDGEMENTS

We thank William Zhang for many useful discussions and providing a NuSTAR flight spare mirror for testing purposes. This work has been financially supported by NASA APRA grant NNX14AE76G and the MIT Kavli Institute Research Investment Fund. Brandon Chalifoux was partially supported by an NSF graduate research fellowship.

REFERENCES

[1] M.C. Weisskopf, J. Gaskin, H. Tananbaum, A. Vikhlinin, "Beyond Chandra: the x-ray Surveyor," Proc. SPIE 9510, EUV and X-ray Optics: Synergy between Laboratory and Space IV, 951002 (2015).

[2] S.L. O'Dell, T.L. Aldcroft, R. Allured, C. Atkins, D.N. Burrows, J. Cao, B.D. Chalifoux, K.-W. Chan, V. Cotroneo, R.F. Elsner, M.E. Graham, M.V. Gubarev, R.K. Heilmann, R.L. Johnson-Wilke, K. Kilaru, J.J. Kolodziejczak, C.F. Lillie, S. McMuldroch, B.D. Ramsey, P.B. Reid, R.E. Riveros, J.M. Roche, T.T. Saha, M.L. Schattenburg, D.A. Schwartz, S.E. Trolier-McKinstry, M.P. Ulmer, S. Vaynman, A. Vikhlinin, X. Wang, M.C. Weisskopf, R.H.T. Wilke, W.W. Zhang, "Toward large-area sub-arcsecond x-ray telescopes ," Proc. SPIE 9208, Adaptive X-Ray Optics III, 920805 (2014).

[3] W.W. Zhang, M.P. Biskach, V.T. Bly, J.M. Carter, K.W. Chan, J.A. Gaskin, M. Hong, B.R. Hohl, W.D. Jones, J.J. Kolodziejczak, L.D. Kolos, J.R. Mazzarella, R.S. McClelland, K.P. McKeon, T.M. Miller, S.L. O'Dell, R.E. Riveros, T.T. Saha, M.J. Schofield, M.V. Sharpe, H.C. Smith, "Affordable and lightweight high-resolution x-ray optics for astronomical missions," Proc. SPIE 9144, Space Telescopes and Instrumentation 2014: Ultraviolet to Gamma Ray, 914415 (2014).

[4] M.J. Collon, M. Ackermann, R. Günther, A. Chatbi, G. Vacanti, M. Vervest, A. Yanson, M.W. Beijersbergen, M. Bavdaz, E. Wille, J. Haneveld, M.O. Riekerink, A. Koelewijn, C. van Baren, P. Müller, M. Krumrey, V. Burwitz, G. Sironi, M. Ghigo, "Making the ATHENA optics using silicon pore optics," Proc. SPIE 9144, Space Telescopes and Instrumentation 2014: Ultraviolet to Gamma Ray, 91442G (2014).

[5] O. Citterio, M. M. Civitani, G. Pareschi, S. Basso, S. Campana, P. Conconi, M. Ghigo, E. Mattaini, A. Moretti, G. Parodi, G. Tagliaferri, "Thin fused silica optics for a few arcsec angular resolution and large collecting area x-ray telescope," Proc. SPIE 8861, Optics for EUV, X-Ray, and Gamma-Ray Astronomy VI, 88610V (2013).

[6] S.L. O'Dell, C. Atkins, D.M. Broadway, R.F. Elsner, J.A. Gaskin, M.V. Gubarev, K. Kilaru, J.J. Kolodziejczak, B.D. Ramsey, J.M. Roche, D.A. Swartz, A.F. Tennant, M.C. Weisskopf, V.E. Zavlin, "X-ray optics at NASA Marshall Space Flight Center," Proc. SPIE 9510, EUV and X-ray Optics: Synergy between Laboratory and Space IV, 951003 (2015).

[7] S. Romaine, R. Bruni, B. Choi, C. Jensen, K. Kilaru, B. Ramsey, S. Sampath, "Development of light weight replicated x-ray optics, II," Proc. SPIE 9144, Space Telescopes and Instrumentation 2014: Ultraviolet to Gamma Ray, 91441H (2014).

[8] R.S. McClelland, M.P. Biskach, K.-W. Chan, R.A. Espina, B.R. Hohl, E.A. Matson, T.T. Saha, W.W. Zhang, "Design, construction, and testing of lightweight x-ray mirror modules," Proc. SPIE 8861, Optics for EUV, X-Ray, and Gamma-Ray Astronomy VI, 88610O (2013).

[9] W.W. Zhang, M.P. Biskach, P.N. Blake, V.T. Bly, J.M. Carter, K.W. Chan, J.A. Gaskin, M. Hong, B.R. Hohl, W.D. Jones, J.J. Kolodziejczak, L.D. Kolos, J.R. Mazzarella, R.S. McClelland, K.P. McKeon, T.M. Miller, S.L. O'Dell, R.E. Riveros, T.T. Saha, M.J. Schofield, M.V. Sharpe, H.C. Smith, "High resolution and high throughput x-ray optics for future astronomical missions," Proc. SPIE 8861, Optics for EUV, X-Ray, and Gamma-Ray Astronomy VI, 88610N (2013).

[10] M. Civitani, S. Basso, M. Ghigo, G. Pareschi, B. Salmaso, D. Spiga, G. Tagliaferri, G. Vecchi, V. Burwitz, G. D. Hartner, B. Menz, "X-ray optical units made of glass: achievements and perspectives," Proc. SPIE 9144, Space Telescopes and Instrumentation 2014: Ultraviolet to Gamma Ray, 914416 (2014).

[11] A. Winter, E. Breunig, P. Friedrich, L. Proserpio, "Progress on indirect glass slumping for future x-ray telescope optics," Proc. SPIE 9144, Space Telescopes and Instrumentation 2014: Ultraviolet to Gamma Ray, 91441C (2014).

[12] W.W. Craig, H.J. An, K.L. Blaedel, F.E. Christensen, T.A. Decker, A. Fabricant, J. Gum, C.J. Hailey, L. Hale, C.B. Jensen, J.E. Koglin, K. Mori, M. Nynka, M.J. Pivovaroff, M.V. Sharpe, M. Stern, G. Tajiri, W.W. Zhang, "Fabrication of the NuSTAR flight optics," Proc. SPIE. 8147, Optics for EUV, X-Ray, and Gamma-Ray Astronomy V, 81470H (2011).

[13] D.M. Broadway, J. Weimer, D. Gurgew, T. Lis, B.D. Ramsey, S.L. O'Dell, M. Gubarev, A. Ames, R. Bruni, "Achieving zero stress in iridium, chromium, and nickel thin films," Proc. SPIE 9510, EUV and X-ray Optics: Synergy between Laboratory and Space IV, 95100E (2015).

[14] W.W. Zhang, "Manufacture of mirror glass substrates for the NuSTAR mission," Proc. SPIE 7437, Optics for EUV, X-Ray, and Gamma-Ray Astronomy IV, 74370N (2009).

[15] E. Sung, B. Chalifoux, M.L. Schattenburg, R.K. Heilmann, "Non-touch thermal air-bearing shaping of x-ray telescope optics," Proc. SPIE 8861, Optics for EUV, X-Ray, and Gamma-Ray Astronomy VI, 88610T (2013).

[16] B. Chalifoux, R.K. Heilmann, M.L. Schattenburg, “Shaping of thin glass X-ray telescope mirrors using air bearing slumping and ion implantation,” Proc. SPIE 9144, Space Telescopes and Instrumentation 2014: Ultraviolet to Gamma Ray, 91444D (2014).

[17] B. Chalifoux, E. Sung, R.K. Heilmann, M.L. Schattenburg, “High-precision figure correction of x-ray telescope optics using ion implantation,” Proc. SPIE 8861, Optics for EUV, X-Ray, and Gamma-Ray Astronomy VI, edited by S.L. O'Dell and G. Pareschi, 88610R (2013).

[18] P.B. Reid, T.L. Aldcroft, R. Allured, V. Cotroneo, R.L. Johnson-Wilke, V. Marquez, S. McMuldroch, S.L. O'Dell, B.D. Ramsey, D.A. Schwartz, S.E. Trolier-McKinstry, A.A. Vikhlinin, R.H.T. Wilke, R. Zhao, “Development status of adjustable grazing incidence optics for 0.5 arcsecond x-ray imaging,” Proc. SPIE 9208, Adaptive X-Ray Optics III, 920807 (2014).

[19] C.R. Forest, C.R. Canizares, D.R. Neal, M. McGuirk, A.H. Slocum and M.L. Schattenburg “Metrology of thin transparent optics using Shack-Hartmann wavefront sensing,” *J. Optical Engineering* **43**, 742-753 (2004).